

Flow and heat transfer in pressing of glass products

Citation for published version (APA):

Laevsky, K., Linden, van der, B. J., & Mattheij, R. M. M. (1999). *Flow and heat transfer in pressing of glass products*. (RANA : reports on applied and numerical analysis; Vol. 9943). Technische Universiteit Eindhoven.

Document status and date:

Published: 01/01/1999

Document Version:

Publisher's PDF, also known as Version of Record (includes final page, issue and volume numbers)

Please check the document version of this publication:

- A submitted manuscript is the version of the article upon submission and before peer-review. There can be important differences between the submitted version and the official published version of record. People interested in the research are advised to contact the author for the final version of the publication, or visit the DOI to the publisher's website.
- The final author version and the galley proof are versions of the publication after peer review.
- The final published version features the final layout of the paper including the volume, issue and page numbers.

[Link to publication](#)

General rights

Copyright and moral rights for the publications made accessible in the public portal are retained by the authors and/or other copyright owners and it is a condition of accessing publications that users recognise and abide by the legal requirements associated with these rights.

- Users may download and print one copy of any publication from the public portal for the purpose of private study or research.
- You may not further distribute the material or use it for any profit-making activity or commercial gain
- You may freely distribute the URL identifying the publication in the public portal.

If the publication is distributed under the terms of Article 25fa of the Dutch Copyright Act, indicated by the "Taverne" license above, please follow below link for the End User Agreement:

www.tue.nl/taverne

Take down policy

If you believe that this document breaches copyright please contact us at:

openaccess@tue.nl

providing details and we will investigate your claim.

EINDHOVEN UNIVERSITY OF TECHNOLOGY
Department of Mathematics and Computing Science

RANA 99-43
December 1999

Flow and heat transfer
in pressing of glass products

by

K. Laevsky, B.J. van der Linden, R.M.M. Mattheij



Reports on Applied and Numerical Analysis
Department of Mathematics and Computing Science
Eindhoven University of Technology
P.O. Box 513
5600 MB Eindhoven, The Netherlands
ISSN: 0926-4507

Flow And Heat Transfer In Pressing Of Glass Products

K. Laevksy, B.J. van der Linden, R.M.M. Mattheij
Department of Mathematics and Computer Science,
Eindhoven University of Technology,
PO Box 513, 5600 MB The Netherlands

November 24, 1999

Abstract

In studying glass morphology often models are used that describe it as a strongly viscous Newtonian fluid. In this paper we shall study one of the problems encountered in glass technology. It is dealing with producing packing glass by a so-called pressing process. The pressing problem actually deals with the morphology of a bottle or jar. We first show how to deal with the temperature, by a suitable dimension analysis. In this analysis we see the dominance of the convection over the other modes of heat transfer. However, at the end of the pressing — a stage called *the dwell* — flow is absent and we have to deal with conduction and radiation in a heat-only problem. A similar analysis is made for the *re-heating*, where the internal stresses are relaxed before the final, blowing stage of the forming process. We give a number of numerical examples to sustain our results.

1 Introduction

For many years, glass technology has been a craft based on expertise and experimental knowledge, reasonably sufficient to keep the products and production competitive. Over the last twenty years mathematical modelling of the various aspects of production has become increasingly decisive, however. This is induced in part by fierce competition from other materials, notably polymers, which, e.g., have found their way into the food packing industry. For another, this is a consequence of environmental concerns. It is not so much the waste (glass is 100% recyclable, a strong advantage to most competitors) as the energy consumption. One should realize that the melting process of sand to liquid glass makes up the largest cost factor of the product. The relative importance of the current industry is illustrated by the following numbers: In the European Union about 25 megatons of glass is being produced, which represents fifty billion euro worth. The industry employs more than 200,000 people. Two-thirds of the glass production is meant for packing (jars

and bottles). Float glass (used for panes) makes up most of the other quarter. The rest is for special products like CRTs and fibers.

Production of container glass products goes more or less along the following lines. First grains of silica (typically available in the form of sand) and additives, like soda, are heated in a tank. This can be an enormous structure with a typical length of several tens of meters and a width of a couple of meters. The height is less impressive and rarely exceeds one meter. Gas burners or electrode heaters provide the necessary heat to heat the material to around 1400°C. At one end, the liquid glass comes out and is either led to a pressing or blowing machine or it ends up on a bed of liquid tin, where it spreads out to become float glass (panes, wind-shields, etc.). In the latter case the major problems are the need for a smooth flow from the oven on the bed and controlling the spreading and flattening. The pressing and blowing process is used in producing packing glass. To obtain a glass form a two-stage process is often used: First a blob of hot glass is pressed into a mould to form a so-called *parison*. It is cooled down (the mould is kept at 500°C) such that a small skin of solid glass is formed. The parison is then blown into its final shape. Such pressing/blowing machinery can produce a number of products at the same time; as a result a more or less steady flow of glass products is coming out on a belt. The products then have to be cooled down in a controlled way such that the remaining stresses are as small as possible (and thus the strength is optimal).

Sometimes only pressing is needed. This is the case in the production of CRTs, where a stamp is pressed into liquid glass and after being lifting, a certain morphology should have been transferred onto the glass screen.

All these processes involve the flow of the (viscous) glass in combination with heat exchange. Although these two are closely intertwined we shall show in this paper that in they can often be decoupled. In cases where convective heat transfer is predominant this effectively leads to isothermal flow problems on one hand and temperature problems on the other. In the stages where flow is absent or negligible we are left with a pure heat problem.

This paper is written as follows. In Section 2 we shall derive the basic flow equations that will play a role in our models. We discuss the pressing of glass in a mould. We describe the model and pay special attention to the heat exchange problem. In Section 3 we discuss the actual pressing phase of the process. In Sections 4 and 5 we look at the post-pressing treatments of the parison: the dwell and the re-heating; these two stages do not involve convection and allow for a thorough treatment of the underlying heat problem.

2 Modelling The Problem

In many cases the process of glass production consists of three main phases. The first one is the pressing phase, the second is the re-heating phase, and the final one the blowing phase. In this section we first describe the process as it is used in industry. The different stages of the process are shown in Figures 2.1 and 2.2. Throughout this section we refer to these figures.

1. A gob of glass leaving the furnace (tank), enters into a configuration consisting of two parts: the mould and the plunger (a). Then, the pressing of the glass takes place in the following

way. The plunger moves up inside of the mould (b) and forces the glass to fill the free space in between. At the end of this stage the glass is left in the mould for a second (c), which is called the *dwelt*. Stages (a), (b) and (c) form the *pressing phase*.

2. After the dwell the *parison* — as the half-product is called — is taken out of the mould and left outside for a couple of seconds (d) giving it the possibility to *re-heat*, i.e. soften the internal temperature gradients.
3. The parison is then placed into a second mould (e) and is blown in to its final shape (f). The latter two stages form the *blowing phase* of the press-and-blow process.

In order to make a sufficient mathematical model of the process it is necessary to mention the basic characteristics and numerical parameters of the process:

$\eta_0 = \eta(T_g) = 10^4 \text{ kg/m s}$	–	the dynamic viscosity of the glass	
$\kappa = 3.50 \text{ m}^{-1}$	–	absorption coefficient	
$\rho = 2500 \text{ kg/m}^3$	–	the density of glass	
$c_p = 1350.0 \text{ J/kg K}$	–	specific heat	
$k^c = 1.71 \text{ W/m K}$	–	conductivity	
$L_0 = 10^{-2} \text{ m}$	–	the typical scale for the parison	(2.1)
$n = 1.50$	–	refractive index	
$T_g = 1250^\circ\text{C}$	–	the temperature of the glass	
$T_m = 700^\circ\text{C}$	–	the temperature of the mould	
$T_p = 1000^\circ\text{C}$	–	the temperature of the plunger	
$V_0 = 10^{-1} \text{ m/s}$	–	the typical velocity of the plunger	

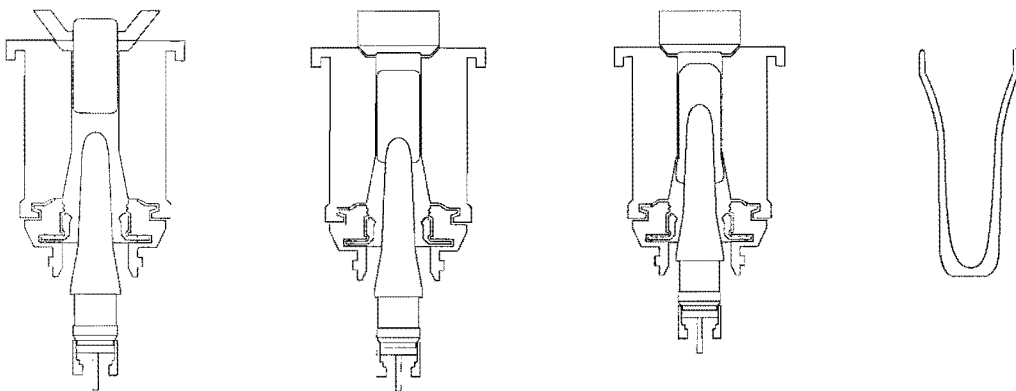


Figure 2.1: The various stages of the pressing phase in a press and blow process: a) The glass enters the mould; b) The plunger presses the glass into form; c) During the dwell the outside of the glass is cooled and solidified; d) The plunger is reheated to reduce temperature gradients.

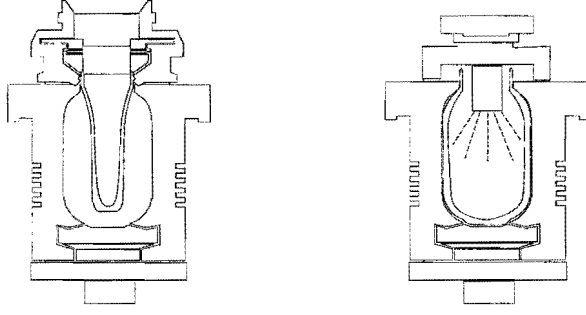


Figure 2.2: The various stages of the blowing phase: e) The plunger is put into the blow mould; f) The glass is blown into its final stage.

2.1 Modelling of The Flow

As it was already implicitly assumed above, the glass — at sufficiently high temperatures — can be considered a viscous fluid. Glass may be viewed as a frozen liquid, i.e. it has an amorphous structure. At sufficiently high temperatures (say above 600 °C) it behaves like an incompressible Newtonian fluid, which means that for a given dynamic viscosity η , a velocity \mathbf{v} and a pressure p , the stress tensor σ is given by

$$\sigma = -p\mathbf{I} + \eta(\nabla\mathbf{v} + \nabla\mathbf{v}^T) \quad (2.2)$$

This constitutive relation should be used to close the equations that actually describe the motion of glass gob, the momentum equation (2.3) and the continuity equation (2.4):

$$\rho \left(\frac{\partial\mathbf{v}}{\partial t} + (\nabla\mathbf{v})^T\mathbf{v} \right) = \rho\mathbf{f} + \nabla \cdot \sigma, \quad (2.3)$$

where ρ denotes the mass density and \mathbf{f} the volume forces on the blob,

$$\nabla \cdot \mathbf{v} = 0. \quad (2.4)$$

Using (2.2) in (2.3) we obtain

$$\rho \left(\frac{\partial\mathbf{v}}{\partial t} + (\nabla\mathbf{v})^T\mathbf{v} \right) = \rho\mathbf{f} - \nabla p + \nabla \cdot [\eta(\nabla\mathbf{v} + \nabla\mathbf{v}^T)] \quad (2.5)$$

In the problem we shall study in this paper we anticipate the viscous forces ($\nabla \cdot \sigma$) to dominate in (2.3). To see this we shall reformulate our equations in dimensionless form, for which we need some characteristic quantities.

First we remark that the only acting volume force in the process is gravity, so $\|\mathbf{f}\| = g \approx 10 \text{ m/s}^2$. We define

$$\tilde{\mathbf{f}} := \frac{1}{g}\mathbf{f}. \quad (2.6)$$

For a fixed temperature, the viscosity η is assumed constant, say $\eta_0 \approx 10^4$ kg/m s for a reference temperature of 800°C. Normally, there is no need to introduce a dimensionless viscosity, but we shall nevertheless do this, as will become clear in the subsequent sections. Thus, let

$$\tilde{\eta} := \frac{1}{\eta_0} \eta. \quad (2.7)$$

A typical average velocity V_0 (which is 10^{-1} m/s or much smaller), say $V_0 \approx 10^{-1}$ m/s, can be used as a characteristic velocity. As a characteristic length scale we take $L_0 (\approx 10^{-2}$ m). We now define the dimensionless quantities

$$\tilde{\mathbf{x}} := \frac{\mathbf{x}}{L_0}, \quad \tilde{\mathbf{v}} := \frac{\mathbf{v}}{V_0}, \quad \tilde{p} := \frac{L_0}{\eta_0 V_0} p. \quad (2.8)$$

A proper choice for characteristic time scale is the ratio $L_0/V_0 (\approx 10^{-1}$ s). So, let us finally define

$$\tilde{t} := \frac{V_0}{L_0} t. \quad (2.9)$$

In this problem the Reynolds number (Re) and the Froude number (Fr), defined by

$$\text{Re} := \frac{V_0 L_0 \rho}{\eta_0}, \quad \text{Fr} := \frac{\rho g L_0^2}{\eta_0 V_0}$$

— an important characteristics. The Reynolds number indicates the ratio between inertial forces and viscous forces and the quotient of the Reynolds number and the Froude number indicates the ratio between volume forces (i.e. gravity) and viscous forces. The two numbers are estimated by

$$\text{Re} \approx 10^{-4}, \quad \text{Fr} \approx 10^{-3}. \quad (2.10)$$

Substituting all dimensionless quantities into (2.4), (2.5) yields

$$\text{Re} \left(\frac{\partial \tilde{\mathbf{v}}}{\partial \tilde{t}} + (\nabla \tilde{\mathbf{v}})^T \tilde{\mathbf{v}} \right) = \text{Fr} \tilde{\mathbf{f}} - \nabla \tilde{p} + \nabla \cdot [\tilde{\eta} (\nabla \tilde{\mathbf{v}} + \nabla \tilde{\mathbf{v}}^T)] \quad (2.11)$$

$$\nabla \cdot \tilde{\mathbf{v}} = 0$$

All spatial derivatives in (2.11) have to be taken with respect to the dimensionless variable $\tilde{\mathbf{x}}$. From this we conclude that the viscous forces dominate indeed. Thus, the equations describing the flow are (rewritten in their dimensionless form)

$$\nabla p = \nabla \cdot [\eta (\nabla \mathbf{v} + \nabla \mathbf{v}^T)] \quad (2.12)$$

$$\nabla \cdot \mathbf{v} = 0$$

These equations are of course the *Stokes creeping flow equations*. They require further boundary conditions in order to be able to solve for the vector \mathbf{v} . Actually, these will be kinematic constraints, changing with time t , describing the evolution of the gob. They have in common that at

least one part of the boundary is free. Hence, besides finding the velocity $\mathbf{v}(t)$ we then need to find this free boundary. The actual displacements \mathbf{x} satisfy the ordinary differential equation:

$$\frac{d\mathbf{x}}{dt} = \mathbf{v}(\mathbf{x}). \quad (2.13)$$

Numerically we shall deal with these problems in a two stage sweep: Suppose we have a domain $\mathcal{G}(t)$, describing the glass gob. Then solve (2.12) (approximately) and use the velocity field on the boundary to compute a new domain at time $t + \Delta t$, using (2.13) and the boundary conditions.

The results of particular simulation, velocity magnitude and pressure field, are depicted on Figure 3.1.

2.2 Modelling of The Heat

The energy equation for an incompressible fluid is given by

$$\rho c_p \frac{DT}{Dt} = -\nabla \cdot \mathbf{q} + \Phi, \quad (2.14)$$

where the heat flux \mathbf{q} is due to the heat transfer mechanisms of conduction and radiation, and the source term Φ comes from the internal heat generation by action of viscous and volume forces. Because of the elevated temperatures in this process and the *semi-transparency* of glass — it absorbs, emits and transmits radiative energy — knowledge of radiation is necessary. Because of the high temperatures and the importance of radiation the heat flux, differently from the usual formulations of the energy equation, consists of a conductive heat flux \mathbf{q}^c and a radiative heat flux \mathbf{q}^r , or

$$\mathbf{q} = \mathbf{q}^c + \mathbf{q}^r. \quad (2.15)$$

During the rest of the analysis we assume that all material properties are constant throughout the medium and time. Furthermore, we assume that the conduction obeys Fourier's law, which states that

$$\mathbf{q}^c := -k^c \nabla T, \quad (2.16)$$

where k^c is the *conductivity*, a material property.

The radiative heat flux cannot be expressed as simply. An approach generally made in industry is to make the often not sustainable assumption that the problem is *optically thick*. This means that the optical thickness τ — defined by $\tau := \kappa L$, where κ is the *absorption coefficient*, which denotes the amount of radiative energy absorbed by the medium per meter, and L is a characteristic length — is much greater than one. For typical values of $\kappa \sim 100\text{m}^{-1}$ for dark glasses, and $L \sim 0.01$ (the thickness of the parison), we see that this assumption is violated. The results later in this section show the lamentable effect this has on the accuracy of the solution.

The reason to make this assumption in practice is made anyway, is that radiation can be accounted for in a computationally cheap way. Especially in higher dimensions, the only other options are:

- Not to account for radiation — and as we have seen in the previous chapter, radiation sometimes plays only a very minor role, even at elevated temperatures;
- To use higher order approximations — in general these are computationally very intensive, e.g. Monte Carlo methods, Modified Diffusion, Ray Tracing.

However, if we restrict ourselves to one dimension we can use both the optically thick method and the exact solution to the heat problem (2.14), and see if there are significant shortcomings with the use of the optically thick approximation.

The derivation of the optically thick approximation — also called the *Rosseland* or *diffusion approximation* — can be found in many text books on radiative heat transfer such as [5] and [1]. Here, we only state the result. The radiative heat flux under this approximation can be written as

$$\mathbf{q}^r := -k^r(T)\nabla T, \quad (2.17)$$

which resembles the expression for the conductive heat flux (2.16). In this equation $k^r(T)$ is called the *Rosseland* parameter and is given by

$$k^r(T) := \frac{4n^2\bar{\sigma}T^3}{3\kappa},$$

where n is the refractive index (a material property) and $\bar{\sigma}$ is the Stefan-Boltzmann constant. We see that the only difference with the conductive heat flux is the non-linearity of the diffusion coefficient. In many applications this can be implemented without a drastic change of the existing code.

For an exact solution we need to go deeper into the theory behind radiative heat transfer. The emitted radiative energy by a medium is proportional to the *total blackbody intensity* $B(T)$, which by definition is the amount of energy per unit area, per unit spherical angle of a perfect emitter-absorber. Because it is already implicitly integrated over all wavelengths, the total blackbody intensity is only a function of the temperature T . Planck found this upper limit to emission to be

$$B(T) = n^2 \frac{\bar{\sigma} T^4}{\pi}. \quad (2.18)$$

Because of the T^4 term, radiation becomes progressively more important than conduction. We will also use the notation $B(\mathbf{x})$, defined as $B(\mathbf{x}) := B(T(\mathbf{x}))$, where the blackbody is a function of the position \mathbf{x} .

In practice most of the other radiative quantities are dependent on the wavelength λ of the radiation, but here we consider so-called *gray radiation*, where this dependence is absent. So, we can define the *radiative intensity* $I(\mathbf{x}, \mathbf{s})$ which is defined as the amount of radiative energy per unit area, per unit solid angle, at a certain position \mathbf{x} , travelling in a certain direction \mathbf{s} . If the radiation is unpolarised and a local thermal equilibrium can be assumed (see [3]), this quantity solely and totally describes electromagnetic radiation. The behaviour of the radiative intensity is determined by the *radiative transfer equation*:

$$\mathbf{s} \cdot \nabla I(\mathbf{x}, \mathbf{s}) = \kappa(\mathbf{x})B(\mathbf{x}) - \kappa(\mathbf{x})I(\mathbf{x}, \mathbf{s}), \quad (2.19)$$

where κ is the *absorption coefficient* denoting the amount of radiative energy absorbed by the medium per unit length. The boundary conditions for this equation for diffusely emitting/reflecting boundaries are given by

$$I(\mathbf{x}_w, \mathbf{s}) = \epsilon(\mathbf{x}_w)B(\mathbf{x}_w) + \frac{\rho(\mathbf{x}_w)}{\pi} \int_{\mathbf{n} \cdot \mathbf{s}' < 0} I(\mathbf{x}_w, \mathbf{s}') \mathbf{n} \cdot \mathbf{s}' d\Omega', \quad \forall \mathbf{s} \cdot \mathbf{n} > 0. \quad (2.20)$$

Here, we used $\epsilon(\mathbf{x}_w)$ for the *emissivity* of the boundary, where \mathbf{x}_w is an arbitrary point on the boundary. Further, $\rho(\mathbf{x}_w)$ is the (*diffuse*) *reflectivity*. Both are material properties. Finally, \mathbf{n} is the outward pointing normal at the boundary.

Then, if we know the intensity, we can determine the radiative heat flux \mathbf{q}^r by

$$\mathbf{q}^r(\mathbf{x}) = \int_{4\pi} \mathbf{s} I(\mathbf{x}, \mathbf{s}) d\Omega. \quad (2.21)$$

In higher dimensions, it is very elaborate to work with these equations. However, a lot can be said about the behaviour of radiative heat transport if we restrict ourselves to one dimension only. The radiative transfer equation (2.19) can be simplified for the quasi-one-dimensional case into the following equations. Here, we mean by quasi-one-dimensional that we do not restrict the *directions* to one dimension. Doing so would result in Rosseland-like solutions. So, let

$$\tilde{\mu} \frac{\partial I^+}{\partial \tau}(\tau, \tilde{\mu}) + I^+(\tau, \tilde{\mu}) = B(\tau), \quad (2.22)$$

$$-\tilde{\mu} \frac{\partial I^-}{\partial \tau}(\tau, \tilde{\mu}) + I^-(\tau, \tilde{\mu}) = B(\tau), \quad (2.23)$$

where I^+ and I^- denote the intensity, $\tau = \int_x \kappa(x) dx$ is the dimensionless optical co-ordinate, and $\tilde{\mu} = |\cos \vartheta|$, where ϑ is the angle of the direction vector with the x -axis. Here we wrote the intensity in two different components I^+ and I^- with a $\tilde{\mu} \in (0, 1]$, because it simplifies relations that follow.

If we look at the problem on the open interval $x \in (x_0, x_1)$, with corresponding dimensionless optical co-ordinate $\tau \in (0, \tau_1)$, the formal solution for the above equations is:

$$I^+(\tau, \tilde{\mu}) = c_0 e^{-\tau/\tilde{\mu}} + \frac{1}{\tilde{\mu}} \int_0^\tau e^{(s-\tau)/\tilde{\mu}} B(s) ds; \quad (2.24)$$

$$I^-(\tau, \tilde{\mu}) = c_1 e^{-\tau/\tilde{\mu}} + \frac{1}{\tilde{\mu}} \int_\tau^{\tau_1} e^{(\tau-s)/\tilde{\mu}} B(s) ds. \quad (2.25)$$

Integrated over all directions these give the two *hemispherical* fluxes q^+ and q^- , defined by

$$q^+(\tau) := 2\pi \int_0^1 \tilde{\mu} I^+(\tau, \tilde{\mu}) d\tilde{\mu} = 2\pi c_0 E_3(\tau) + 2\pi \int_0^\tau E_2(\tau - s) B(s) ds; \quad (2.26)$$

$$q^-(\tau) := 2\pi \int_0^1 \tilde{\mu} I^-(\tau, \tilde{\mu}) d\tilde{\mu} = 2\pi c_1 E_3(\tau_1 - \tau) + 2\pi \int_\tau^{\tau_1} E_2(\tau - s) B(s) ds, \quad (2.27)$$

where E_i is the i -th exponential integral. Then, we can construct the radiative heat flux with

$$q^r := 2\pi \int_0^1 \tilde{\mu} [I^+(\tau, \tilde{\mu}) - I^-(\tau, \tilde{\mu})] d\tilde{\mu} = q^+ - q^-. \quad (2.28)$$

Combining (2.26–2.28) then gives

$$q^r = 2\pi c_0 E_3(\tau) + 2\pi \int_0^\tau E_2(\tau - s) B(s) ds - 2\pi c_1 E_3(\tau_1 - \tau) - 2\pi \int_\tau^{\tau_1} E_2(s - \tau) B(s) ds, \quad (2.29)$$

Since in the heat equations we use the gradient of the heat flux, we differentiate (2.29) immediately to find

$$\frac{dq^r}{d\tau}(\tau) = 4\pi B(\tau) - 2\pi c_0 E_2(\tau) - 2\pi c_1 E_2(\tau_1 - \tau) - 2\pi \int_0^{\tau_1} E_1(|\tau - s|) B(s) ds. \quad (2.30)$$

In this equation c_0 and c_1 are still undetermined; they are depending on the radiative properties of the boundaries, which we have silently assumed to be diffusely emitting and reflecting. The case with no reflection — $\rho = 0$ in (2.20) — is the simplest. Because of Kirchhoff's law:

$$\epsilon + \rho = 1, \quad (2.31)$$

we find that $\epsilon = 1$; in other words we are dealing with perfectly black walls and the emitted intensities at the boundaries are equal to the blackbody intensity. As we will see in the Section 5, this situation applies in the reheating phase when the parison is situated in an infinite atmosphere.

However, for the dwell this is not valid. During the dwell the glass is enclosed by the metal mould on both ends and metal typically has a reflectivity of $\rho \approx 0.9$. Therefore we must have a closer look of (2.20), which rephrased for one dimension and integrated over the right directions reads

$$2\pi c_0 := q^+(0) = 2\pi \epsilon_0 B_0 + \rho_0 q^-(0); \quad (2.32)$$

$$2\pi c_1 := q^-(\tau_1) = 2\pi \epsilon_1 B_1 + \rho_1 q^+(\tau_1). \quad (2.33)$$

Here B_0 and B_1 are the blackbody intensities due to the temperature of the respective walls, and not due to the temperature of the glass at those walls. If conduction is neglected, it should be noted that there usually is a temperature jump at the boundary. The hemispherical fluxes at the wall have special names: $q_0^+ := q^+(0)$ and $q_1^- := q^-(\tau_1)$ are called the *radiosities* of the respective boundaries, while $q_0^- := q^-(0)$ and $q_1^+ := q^+(\tau_1)$ are called the *irradiation* at those walls. Applying (2.26,2.27) to (2.32,2.33), and then applying the latter two again, gives

$$c_0 = \frac{\epsilon_0 B_0 + \rho_0 \epsilon_1 B_1 E_2(\tau_1) + \rho_0 \int_0^{\tau_1} E_1(s) B(s) ds + \rho_0 \rho_1 E_2(\tau_1) \int_0^{\tau_1} E_1(\tau_1 - s) B(s) ds}{1 - \rho_0 \rho_1 E_2^2(\tau_1)}; \quad (2.34)$$

$$c_1 = \frac{\epsilon_1 B_1 + \rho_1 \epsilon_0 B_0 E_2(\tau_1) + \rho_1 \int_0^{\tau_1} E_1(s) B(\tau_1 - s) ds + \rho_0 \rho_1 E_2(\tau_1) \int_0^{\tau_1} E_1(s) B(s) ds}{1 - \rho_0 \rho_1 E_2^2(\tau_1)}. \quad (2.35)$$

If we know the temperature distribution and the temperature of the walls we can use (2.18) directly to compute c_0 and c_1 from these. Although in most heat problems we do not know the temperature distribution *a priori*, the use of (2.30) together with (2.34,2.35) is next to trivial in explicit or iterative methods.

For higher dimensions a similar but more complex derivation can be done. The method where the Discrete Ordinate Method — described in [4] — and ray tracing are combined to approximate the formal solution. A discussion of this method is beyond the scope of this article. The theory behind it can be found in [7].

3 Pressing phase

As usual in viscous fluid flow the energy equation is ignored because in an incompressible Newtonian fluid with constant viscosity it is not coupled to the equations of motion. In the present case the high viscous forces might generate heat by friction, such that the temperature rises and the viscosity decreases. In order to investigate this possibility consider the energy equation (2.14) for incompressible flow. Using (2.15), (2.16) and (2.17) we can rewrite it as follows:

$$\rho c_p \left(\frac{\partial T}{\partial t} + \mathbf{v} \cdot \nabla T \right) = k^c \nabla^2 T + \nabla \cdot (k^r(T) \nabla T) + \eta ((\nabla \mathbf{v} + \nabla \mathbf{v}^T) : \nabla \mathbf{v}), \quad (3.1)$$

where c_p is the heat capacity, T is the absolute temperature, η is the viscosity, k^c is the heat conductivity, and $k^r(T)$ is the Rosseland parameter as it was defined before.

Let us introduce a dimensionless temperature variable \tilde{T} :

$$T = T_m + \Delta T \tilde{T}, \quad (3.2)$$

where $\Delta T = T_g - T_m$ (T_g , T_m are the temperatures of the glass and the mould, as defined in (2.1)). Using dimensionless variables (2.7), (2.8) and (3.2) the equation above reads as follows

$$\frac{\partial \tilde{T}}{\partial \tilde{t}} + \tilde{\mathbf{v}} \cdot \nabla \tilde{T} = \frac{1}{\text{Pe}} \nabla^2 \tilde{T} + \nabla \cdot \left(\frac{k^r(T)}{k^c} \frac{1}{\text{Pe}} \nabla \tilde{T} \right) + \frac{\text{Ec}}{\text{Re}} \tilde{\eta} ((\nabla \tilde{\mathbf{v}} + \nabla \tilde{\mathbf{v}}^T) : \nabla \tilde{\mathbf{v}}). \quad (3.3)$$

Both the dimensionless numbers $1/\text{Pe}$ and Ec/Re , defined by

$$\text{Pe} := \frac{\rho c_p L_0 V_0}{k^c}, \quad \text{Re} := \frac{V_0 L_0 \rho}{\eta_0}, \quad \text{Ec} := \frac{V_0^2}{c_p \Delta T}$$

are of order 10^{-4} , so the energy equation (3.1) simplifies to:

$$\frac{dT}{dt} = \frac{\partial T}{\partial t} + \mathbf{v} \cdot \nabla T = 0, \quad (3.4)$$

so the temperature remains constant. Thus, assuming uniform temperature distribution in the glass gob, we can compute the flow using correspondent constant viscosity η . As a result velocity and pressure fields can be obtained.

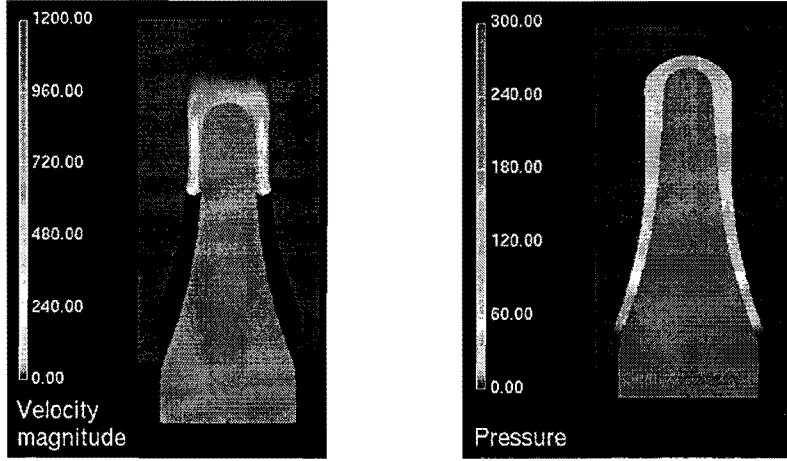


Figure 3.1: Velocity magnitude and pressure field.

4 Dwell

During the dwell — the stage when the glass is kept in the mould after all the air has been forced out — there is no flow. If the radius and the height of the bottle is much bigger than its thickness, as is usually the case, we can locally approximate the behaviour of the temperature as being one dimensional. In this case, the two walls of our approximation in Section 2.2 are the mould on one side and the plunger on the other. It is assumed that the glass makes perfect contact with both the mould and the plunger, so we can assume Dirichlet boundary conditions on either side. The thickness of the glass layer is denoted with L . In this case, (2.14) simplifies to

$$\rho c_p \frac{\partial T}{\partial t} = -\frac{\partial q^c}{\partial x} - \frac{\partial q^r}{\partial x}, \quad t > 0, \quad 0 < x < L; \quad (4.1)$$

to which the following boundary and initial conditions are added:

$$T(t, 0) = T_{\text{mould}}, \quad T(t, L) = T_{\text{parison}}, \quad \text{and} \quad T(0, x) = T_0(x). \quad (4.2)$$

Now, we define the *Rosseland number* Ro to be

$$\text{Ro} := \frac{k^c \kappa}{4n^2 \tilde{\sigma} T_w^3}, \quad (4.3)$$

where T_w is some characteristic temperature (e.g. the temperature of the walls or the average thereof). If we assume optical thickness, the Rosseland approximation (2.17) holds, the ratio between the radiative and conductive diffusion parameters is

$$\frac{k^r}{k^c} = \frac{\vartheta^3}{3\text{Ro}},$$

in which $\vartheta := T/T_w$ is the dimensionless temperature. Remembering we assumed the material properties to be constant, and defining the *thermal diffusivity* to be $\alpha := k^c/\rho c_p$, (4.1) becomes,

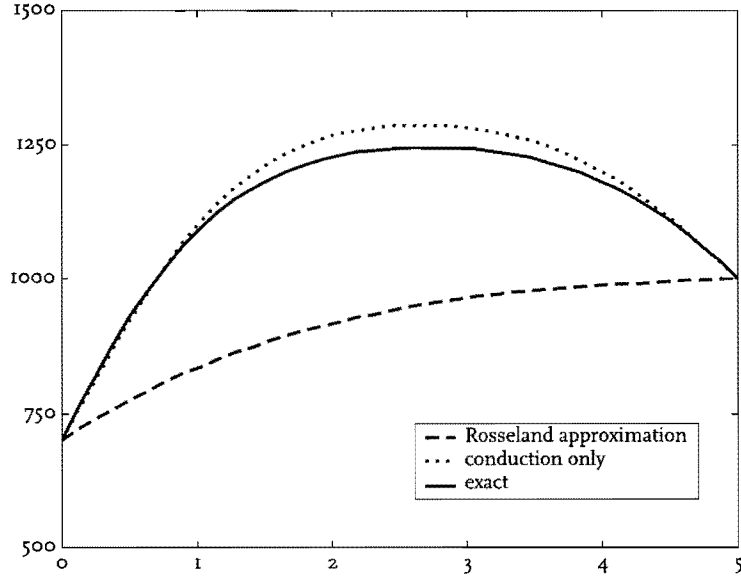


Figure 4.1: Temperature profile after one second dwell (various methods).

after dividing left and righthand side by T_w and k^c :

$$\frac{1}{\alpha} \frac{\partial T}{\partial t} = \frac{\partial}{\partial x} \left[\left(1 + \frac{\vartheta^3}{3\text{Ro}} \right) \frac{\partial T}{\partial x} \right].$$

Introducing the *Fourier number* (dimensionless time) $\varphi := \alpha t / L^2$ and the dimensionless coordinate $\xi := x / L$ this simplifies to, after division by T_w ,

$$\frac{\partial \vartheta}{\partial \varphi} = \frac{\partial}{\partial \xi} \left[\left(1 + \frac{\vartheta^3}{3\text{Ro}} \right) \frac{\partial \vartheta}{\partial \xi} \right]. \quad (4.4)$$

Expressed in the optical coordinate $\tau := \kappa L$ and the *optical Fourier number* $\varphi_r := \alpha \kappa^2 t$, this can be written as:

$$\frac{\partial \vartheta}{\partial \varphi_r} = \frac{\partial}{\partial \tau} \left[\left(1 + \frac{\vartheta^3}{3\text{Ro}} \right) \frac{\partial \vartheta}{\partial \tau} \right]. \quad (4.5)$$

Finally, if we do not use the Rosseland approximation, but some exact method to obtain the radiative flux, we can perform the same coordinate transformations. If we furthermore define the *dimensionless radiative heat flux* to be $Q^r := q^r / 4n^2 \tilde{\sigma} T^4$, we find that

$$\frac{\partial \vartheta}{\partial \varphi_r} = \frac{\partial^2 \vartheta}{\partial \tau^2} - \frac{1}{\text{Ro}} \frac{\partial Q^r}{\partial \tau}. \quad (4.6)$$

Here we can use the method outlined in Section 2.2 to obtain values for the heat flux and its divergence.

In Figure 4.1, we see the results of the one-dimensional problem for a computation simulating a dwell time of one second. The most eye-catching is the erroneous result, the Rosseland approximation gives us in this case. We should have been warned by the small optical thickness (of order one in the production of jars and bottles). This result is worrying as in industry it is widely used ‘just to take care of radiation’. The results here show that far better results are achieved by simply neglecting the radiation. Still, one has to take care, since after longer periods the exact method and the radiation neglecting method will deviate severely, too.

The reason the Rosseland approximation fails here, is that it overestimates the radiative energy transport. The glass is not thick enough to achieve diffusion-like behaviour. The Dirichlet boundary-conditions applied to both boundaries enforce a large gradient of the thin glass sample. It is this gradient that makes the problem conduction driven, aggravating the results of the Rosseland approximation, which is basically enlarging the effective conductivity.

We see from these calculations that for short times (i.e. very small Fourier numbers), the conduction-driven problem can be approached by omission of the radiation. This apparently is still valid for the cases in which the optical thickness τ_1 and Rosseland number do not directly indicate the radiation is not crucially unimportant. Yet, be aware that still significant errors are made by such a simple approximation (maximum 50°C in this example). So, depending on the importance of the temperature and its gradient one can choose between accuracy and speed. In this case, for example, a quite big difference of 50 degrees during the dwell does not give rise to an erroneous prediction of the remainder of the process. Simply omitting the radiation, would therefore be most likely candidate for simulations in more dimensions, where the implementation of the exact method brings severe performance penalties.

5 Reheating phase

The heat problem in the reheating phase is basically the same as during the dwell: only the boundary conditions differ. During reheating the parison is standing outside the mould and without plunger in an open atmosphere. This open atmosphere from an radiative point of view lets itself be accurately modelled as a blackbody, with the ambient temperature as driving force. The contact with the surrounding atmosphere is, unlike during the dwell, not a perfect contact. Rather we have to apply a Robin boundary conditions describing the exchange of heat with this surrounding atmosphere. Since, the *ambient temperature* T_∞ — say standard room temperature (20°C) — is much cooler than the parison, we expect it to act as a heat sink. The infinite surroundings of the parison can be seen as a blackbody boundary as shown in Figure 5.1. On the outside we have both convective and radiative cooling of the parison. The convective heat q_0^{conv} entering the parison on the outside is due to free convection of the surrounding air. It can be calculated by:

$$q_0^{\text{conv}}(t) = h(T_\infty - T(t, 0)), \quad (5.1)$$

where h is the *convective heat transfer coefficient*. Methods to compute this can be found in books like [6]. Typically its value is 1–2W/m².

How the radiative properties are taken into account, depends on the model of radiation that is chosen. For the exact method we calculate the intensity of the atmosphere with (2.18), then (2.34)

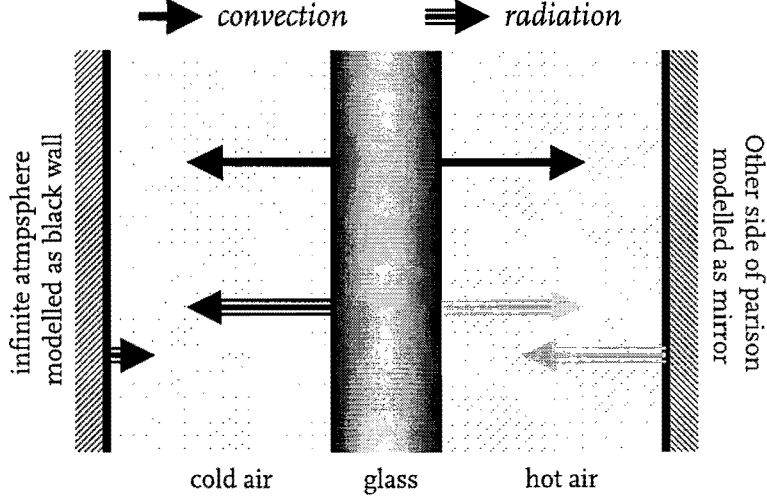


Figure 5.1: The model for the reheating phase. The inner side of the parison ‘sees’ the other side, and thus, the irradiance at this boundary is equal to its radiosity.

leads to $c_0 = n^2 \bar{\sigma} T_\infty^4 / \pi$. This coefficient then is used in (2.30), which we use to calculate the radiative heat flux gradient throughout the glass. If the Rosseland method is used, however, the radiative exchange of the glass with its surroundings can only be applied at the boundary. We find a similar expression to (5.1) that states:

$$q_0^{\text{rad}}(t) = \varepsilon \bar{\sigma} (T_\infty^4 - T(t, 0)^4). \quad (5.2)$$

The emissivity ε , being equal to the absorpsivity, can be determined as follows. Given the intensity B_∞ entering the glass at certain direction $\tilde{\mu}$, it will travel through the glass, then through the inside and then through the glass again. Because the hot air does not absorb, we can see from (2.24) that an intensity of $B_\infty e^{-2\tau_1/\tilde{\mu}}$ caused by the entering radiation, is leaving the glass again. We can now calculate ε using

$$\varepsilon = \frac{2\pi B_\infty - 2\pi \int_0^1 \tilde{\mu} B_\infty e^{-2\tau_1/\tilde{\mu}} d\mu}{2\pi B_\infty} = 1 - 2E_2(2\tau_1).$$

On the inner side of the parison, the convective heat exchange can be modelled as before:

$$q_1^{\text{conv}}(t) = h(T(t, L) - T_{\text{hot}}), \quad (5.3)$$

where T_{hot} is the temperature of the hot air inside the parison. As for the radiative exchange, we do not ‘see’ the surrounding atmosphere (directly), but the other inner side of the parison instead. The radiative boundary condition for this side of the glass can be modelled as specularly reflective. Depending on the radiation model this can be simplified further. If we are using a diffusion approximation all the radiative heat has to leave at boundary. However, since there is a specular wall between the glass and the infinite surroundings of the parison, and since air in absence of

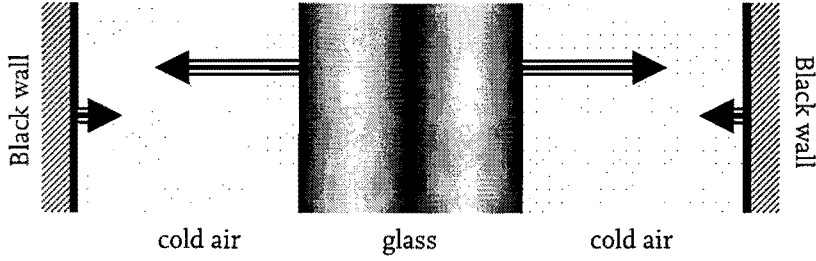


Figure 5.2: Additional model for the reheating phase. The specularly reflective boundary is tackled by reflecting the domain.

high vapour and CO_2 concentrations does not absorb radiative heat, the radiative heat exchange at the surface equals zero.

If we use the exact radiation model, treating specular reflections is even more involved than the diffuse reflection we have seen in Section 2. As shown in Figure 5.2, in one dimension we can evade this, by simply doing what the reflective boundary does: make a reflection. So, rather than using (5.1) over the physical interval $(0, \tau_1)$, we use this equation over the interval $(0, 2\tau_1)$, where we extend the blackbody intensity by using:

$$B(\tau) = B(2\tau_1 - \tau), \quad \forall \tau \in (\tau_1, 2\tau_1). \quad (5.4)$$

The problem is written now almost identical to (4.1); only the boundary conditions are different, as can be seen in

$$\rho c_p \frac{\partial T}{\partial t} = -\frac{\partial q^c}{\partial x} - \frac{\partial q^r}{\partial x}, \quad t > 0, \quad 0 < x < L \quad (5.5)$$

to which the following initial condition is added:

$$T(0, x) = T_0(x). \quad (5.6)$$

The boundary conditions are different for different models. For diffusion models (like the Rosseland model or simple neglect of radiation), we have to include the term for radiative heat loss *at* the boundary. Then, the boundary equation becomes the non-linear Robin-condition

$$\frac{\partial T}{\partial x} = \frac{h}{k^{\text{eff}}} (T_\infty - T(t, 0)) + \frac{\varepsilon \bar{\sigma}}{k^{\text{eff}}} (T_\infty^4 - T(t, 0)^4), \quad (5.7)$$

where k^{eff} is the *effective conductivity*. In the Rosseland approximation this is equal to $(k^c + k^r(T))$, whereas it is simply k^c if we neglect radiation.

If we use the exact method for the radiation, any loss of heat through radiation to its surroundings is already taken care of by the q^r term. The boundary conditions therefore only have to prescribe the convection at the boundaries:

$$\frac{\partial T}{\partial x} = \frac{h}{k^{\text{eff}}} (T_\infty - T(t, 0)) \quad (5.8)$$

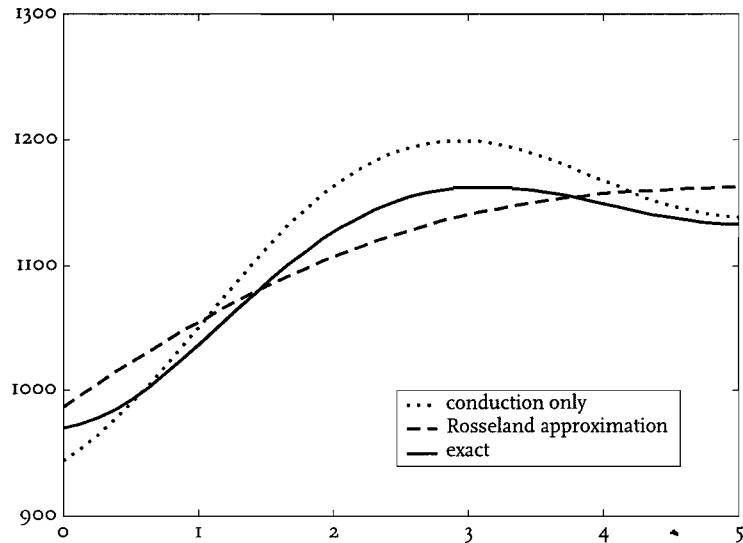


Figure 5.3: Temperature profile after one second dwell (exact method) and one second reheating (various methods).

As we can see in Figure 5.3, more so than during the dwell, the three methods give very different results. Unlike during the dwell, however, the Rosseland approximation now gives a good estimate of the energy being extracted during the reheat. In this case, omission of the radiative heat transfer also leads to large errors, especially concerning the cooling down of the glass. Both simplifications under-perform in approximating the temperature gradients, which are so important during the reheating.

The conclusion is clear. During reheating, in a case where neither the conduction (as in the optical thin case) nor the radiation (as in the optical thick case) is predominant, only an exact approach gives trustworthy results. If it has been identified either the temperature itself or its gradient is critical to the functioning of the process, effort has to be made to get the radiative heat transfer right. Two numbers, the optical thickness τ_1 and the Rosseland number Ro , can assist in determining whether this effort has to be made. From comparison of the results of the dwell and the reheat, however, we see that these two numbers by themselves are not conclusive. The Dirichlet-conditions applied in the dwell, and thus applying a large temperature gradient over a small distance, forced the conduction to be dominant. Natural boundary conditions as during the reheat, however, give value to the two aforementioned numbers.

The results presented were derived for the simple one-dimensional case. In higher dimensions the simplicity of the Rosseland equation becomes even more tempting as the computational complexity of the exact solution raises. For the best approximations of three-dimensional problems methods as the Monte Carlo Method and the Ray Trace Method are utilised. However, the large computational times associated with these methods are usually considered to be prohibitive for implementation in simulations of processes in the production of glass. Newer methods include the algebraic form of the Ray Trace Method, presented in [7], and the *Modified Diffusion Approximation* as discussed in [2]. Given the results presented it here it seems wise to implement a method

other than the (standard) Rosseland approximation for thin to medium optical thicknesses, or to accept that the temperature and temperature gradients of the simulation are plainly inaccurate.

References

- [1] S. CHANDRASEKHAR, *Radiative Transfer*, Dover Publications, Inc., Toronto, 1960.
- [2] F. LENTES AND N. SIEDOW, *Three-dimensional radiative heat transfer in glass cooling processes*, Tech. Rep. Berichte Nr. 4, ITWM, Kaiserslautern, 1998.
- [3] D. MIHALAS AND B. WEIBEL-MIHALAS, *Foundations of Radiation Hydrodynamics*, Oxford University Press, Oxford, 1984.
- [4] M. MODEST, *Radiative Heat Transfer*, McGraw-Hill, Inc., Singapore, 1993.
- [5] M. ÖZİŞİK, *Radiative Transfer and Interactions with Conduction and Convection*, John Wiley and Sons, Inc., Toronto, 1973.
- [6] B. TAPLEY AND T. POSTON, *Eschbach's Handbook Of Engineering Fundamentals, Fourth Edition*, John Wiley and Sons, Inc., Toronto, 1989.
- [7] B. VAN DER LINDEN AND R. MATTHEIJ, *A new method for solving radiative heat problems in glass*, International Journal of Forming Processes, 2 (1999), pp. 41–61.